

Target Acceleration Modeling for Tactical Missile Guidance

Paul L. Vergez* and Randall K. Liefer†

U.S. Air Force Armament Laboratory, Eglin Air Force Base, Florida

For future short-range air-to-air missile concepts, it has been demonstrated that linear optimal guidance laws provide significant performance improvements over proportional navigation guidance laws. This paper addresses the critical problem of estimating the missile-to-target position, velocity, and acceleration (required by the linear optimal guidance law) when only passive (angle only) seeker information is available onboard a highly maneuverable bank-to-turn missile concept. More specifically, the problem is how to model the target acceleration to achieve improved missile performance. Four target acceleration models coupled with an extended Kalman filter are presented and evaluated on a six-degree-of-freedom missile simulation to determine their estimation effectiveness and their influence on missile guidance.

I. Introduction

APPLICATIONS of optimal control theory to the tactical missile guidance problem have drawn much attention in recent years. The most commonly used theory is linear quadratic Gaussian (LQG) theory because it is based on a linear system model and provides a closed-form solution. Further, it has been demonstrated that for the short-range tactical missile, the LQG guidance law provides significant performance improvements over the more commonly used classical proportional navigation guidance laws. Additionally, in terms of future missile performance requirements and future target characteristics, proportional navigation will be inadequate.¹

A critical issue that affects performance of the LQG guidance law is the fact that it is a function of time-to-go (time remaining before intercept) and the missile-to-target position, velocity, and acceleration. Time-to-go is typically estimated from the later information noted in the preceding sentence. Although not the subject of this paper, much work has been accomplished toward improving time-to-go estimates.² Everyone will agree, however, that the estimates of time-to-go and the performance of LQG guidance law are most effective when the required position, velocity, and acceleration information is accurate.

One of the fundamental problems that has limited the practicality of the LQG guidance law is the difficulty in obtaining the accurate state information required. Most present-day missiles can obtain a measure of the missile's acceleration through onboard accelerometers; however, this information is not presently used for guidance purposes. In addition, passive seekers are used to provide a measure of line-of-sight angle and rate. Since proportional navigation (PN) is a function of line-of-sight rate only, a passive seeker is more than adequate. A low-pass filter is typically used to process the noise from the line-of-sight rate for PN. To make use of the LQG guidance law more information is needed.

There are two solutions to obtain the necessary information for the LQG guidance law: one is to increase the accuracy and number of onboard sensors. Cost, size, and weight factors make this solution unattractive. Further, the target acceleration simply cannot be measured. These hardware

problems can be solved potentially through the use of advanced software techniques, which leads to the second solution.

Recent advances in estimation theory, coupled with the explosion in microprocessor technology, make it feasible to develop complex yet realizable estimation algorithms. This new capability could solve the information problem in tactical missile systems without increasing the number and types of sensors currently in use in tactical weapons. This is done in an attempt to minimize hardware requirements for mechanization of advanced high-performance guidance techniques.

The most widely accepted estimation theory is use today is Kalman filtering, which was developed in the early 1960's. Much work has been done in recent years applying this theory to the tactical missile guidance problem, in particular, the use of extended Kalman filters (EKF's).²⁻⁵ Still, a critical design factor in an EKF is the modeling of the target acceleration. It is impossible to model the target acceleration for practical application accurately because one cannot know exactly what a target will do, particularly a flying target.

The purpose of this paper is to present four target acceleration models for an EKF, evaluate their estimation effectiveness, and determine their influence on tactical missile guidance when coupled with an LQG guidance law. The four target acceleration models evaluated are 1) first-order Markov process, 2) second-order Markov process, 3) constant target acceleration, and 4) zero target acceleration.

II. Extended Kalman Filter

It is important to describe first how an extended Kalman filter works, and then present the differences introduced by the four target acceleration models. Figure 1 shows the flow diagram for an extended Kalman filter. Subsections II.A through II.E show the derivation of the algorithms of the EKF for the missile/target intercept problem.

A. State and Measurement Models

State model:

$$\dot{X}(t) = FX(t) + Bu(t) + w(t), \quad w(t) \sim N(0, Q(t))$$

$$X(0) \sim N(X_0, P_0) \quad (1)$$

Measurement model:

$$Z_k = g(X(t_k)) + v_k, \quad v_k \sim N(0, R_k) \quad k = 1, 2, 3, \dots \quad (2)$$

Submitted June 18, 1981; revision received Jan. 3, 1983. This paper is declared a work of the U.S. Government and therefore is in the public domain.

*Captain, USAF, Program Director, Guidance and Control Engineer.

†Captain, USAF, Guidance and Control Engineer.

where

- $X(t)$ = EKF states
- F = state matrix
- $Bu(t)$ = state forcing function
- $w(t)$ = accuracy of states, white Gaussian noise (WGN) with zero mean
- $Q(t)$ = standard deviation of WGN of states
- Z_k = EKF measurements
- v_k = accuracy of measurements, WGN with zero mean
- R_k = standard deviation of WGN of measurements
- X_0 = initial value of states
- P_0 = initial error covariance of states

B. State Transition Matrix

The state transition matrix, along with the forcing function, is used to propagate the filter states and error covariances.

The state transition matrix, $\Phi(t_k, t_{k-1})$, is

$$\Phi(t_k, t_{k-1}) = \mathcal{L}^{-1} (SI - F)^{-1} \quad (3)$$

C. State and Covariance Propagation

The propagation equations of the state estimates (\hat{X}), and error covariances, (\hat{P}), are:

$$\hat{X}(t_k) = \Phi(t_k, t_{k-1}) \hat{X}(t_{k-1}) + \int_{t_{k-1}}^{t_k} \Phi(t_k, \tau) Bu(\tau) d\tau \quad (4)$$

$$\begin{aligned} \hat{P}(t_k) &= \Phi(t_k, t_{k-1}) P(t_{k-1}) \Phi^T(t_k, t_{k-1}) \\ &+ \int_{t_{k-1}}^{t_k} \Phi(t_k, \tau) Q(\tau) \Phi^T(t_k, \tau) d\tau \end{aligned} \quad (5)$$

where $\hat{X}(t_k)$ is the propagated state estimate and $\hat{P}(t_k)$ the propagated error covariance.

D. Kalman Gain Matrix

The Kalman gain matrix, K , is used to minimize the diagonal elements of the error covariance matrix. It is obtained from the following equation.

$$\begin{aligned} K(t_k) &= \hat{P}(t_k) H^T (\bar{X}(t_k)) [H(\bar{X}(t_k)) \hat{P}(t_k) H^T (\bar{X}(t_k)) \\ &+ R(t_k)]^{-1} \end{aligned} \quad (6)$$

where

$$H(\bar{X}(t_k)) = \left. \frac{\partial g(X(t_k))}{\partial X(t_k)} \right|_{X=\bar{X}} \quad (7)$$

E. State and Covariance Updates

The final step is to update the filter states and error covariances in order to drive the errors between the actual measurements and the filter's estimate of the measurements to zero. These updates are obtained from the following equations.

$$\hat{X}(t_k) = X(t_k) + K(t_k) [Z(t_k) - g(\bar{X}(t_k))] \quad (8)$$

$$\hat{P}(t_k) = [I - K(t_k) H(\bar{X}(t_k))] \hat{P}(t_k) \quad (9)$$

III. System Model with First-Order Markov Process

The EKF is set up as a nine-state filter with the system model in Cartesian coordinates. The nine states are the three components of relative position, relative velocity, and target acceleration, all with respect to inertial coordinates. The missile's acceleration is measured onboard and is used as a forcing function of the states.

The differential state equations are:

$$\Delta \dot{S}(t) = \Delta V(t) \quad (10a)$$

$$\Delta \dot{V}(t) = A_T(t) - A_M(t) + w_M(t) \quad (10b)$$

$$\dot{A}_T(t) = \lambda_T A_T(t) + w_T(t) \quad (10c)$$

In state space format, the system model is:

$$\begin{aligned} \begin{bmatrix} \Delta \dot{S}(t) \\ \Delta \dot{V}(t) \\ \dot{A}_T(t) \end{bmatrix}_{9 \times 1} &= \begin{bmatrix} 0 & I & 0 \\ 0 & 0 & I \\ 0 & 0 & -T^I \end{bmatrix}_{9 \times 9} \begin{bmatrix} \Delta S(t) \\ \Delta V(t) \\ A_T(t) \end{bmatrix}_{9 \times 1} \\ &+ \begin{bmatrix} 0 & 0 & 0 \\ 0 & I & 0 \\ 0 & 0 & 0 \end{bmatrix}_{9 \times 9} \begin{bmatrix} 0 \\ A_M(t) \\ 0 \end{bmatrix}_{9 \times 1} + \begin{bmatrix} 0 \\ w_M(t) \\ w_T(t) \end{bmatrix}_{9 \times 1} \end{aligned} \quad (11)$$

where

$\Delta S(t)$ = three components of relative position, ft (inertial coordinate)

$\Delta V(t)$ = three components of relative velocity, ft/s (inertial coordinate)

$A_T(t)$ = three components of target acceleration, ft/s² (inertial coordinate)

$A_M(t)$ = three components of missile acceleration, ft/s² (inertial coordinate)

λ_T = target acceleration response time coefficient, s⁻¹

For the system model in Eq. (11), the state transition matrix [derived from Eq. (3)] is:

$$\Phi(t_k, t_{k-1}) = \begin{bmatrix} I & \Delta t I & \Phi_{13} I \\ 0 & I & \Phi_{23} I \\ 0 & 0 & e^{-\lambda_T \Delta t} I \end{bmatrix}_{9 \times 9} \quad (12)$$

where

$$\Phi_{13} = \frac{e^{-\lambda_T \Delta t} + \Delta t \lambda_T - 1}{\lambda_T \Delta t} \quad (13)$$

$$\Phi_{23} = \frac{1 - e^{-\lambda_T \Delta t}}{\lambda_T} \quad (14)$$

IV. System Model with Second-Order Markov Process

For this model, the three components of relative position remain the same as in Sec. III; however, the target acceleration as a second-order Markov process is a function of target velocity. The nine filter states are now the three components of relative position, target velocity, and target acceleration, all with respect to inertial coordinates. The differential state equations now are:

$$\Delta \dot{S}(t) = V_T(t) - V_M(t) + w'_M(t) \quad (15a)$$

$$\dot{V}_T(t) = A_T(t) \quad (15b)$$

$$\dot{A}_T(t) = -\omega^2(t) V_T(t) + w_T(t) \quad (15c)$$

when $V_M(t)$ is the missile's velocity with respect to inertial coordinates and is obtained by integrating the measured missile acceleration, and $V_T(t)$ is the target's velocity with respect to inertial coordinates. The system model for the EKF

now becomes:

$$\begin{bmatrix} \Delta \dot{S}(t) \\ \Delta \dot{V}(t) \\ \dot{A}_T(t) \end{bmatrix}_{9 \times 1} = \begin{bmatrix} 0 & I & 0 \\ 0 & 0 & I \\ 0 & -\omega^2(t)I & 0 \end{bmatrix}_{9 \times 9} \begin{bmatrix} \Delta S(t) \\ \Delta V(t) \\ A_T(t) \end{bmatrix}_{9 \times 1} + \begin{bmatrix} -I & 0 & 0 \\ 0 & 0 & 0 \\ 0 & 0 & 0 \end{bmatrix}_{9 \times 9} \begin{bmatrix} V_M(t) \\ 0 \\ 0 \end{bmatrix}_{9 \times 1} + \begin{bmatrix} w'_M(t) \\ 0 \\ w_T(t) \end{bmatrix}_{9 \times 1} \quad (16)$$

where

$$\begin{bmatrix} w'_M(t) \\ 0 \\ w_T(t) \end{bmatrix} \sim N(0, Q'(t))$$

with

$$Q'(t) = \begin{bmatrix} \Delta t Q_M & 0 & 0 \\ 0 & 0 & 0 \\ 0 & 0 & Q_T \end{bmatrix}_{9 \times 9} \quad (17)$$

The vector $\omega(t)$ is the three components of target turning rate and is obtained by

$$\omega(t) = \frac{V_T(t) \times A_T(t)}{|V_T(t)|^2} \quad (18)$$

$V_T(t)$ and $A_T(t)$ are the estimated states of the filter. The state transition matrix for the system model, Eq. (16), is

$$\Phi(t_k, t_{k-1}) =$$

$$\begin{bmatrix} I & \frac{\sin \omega(t_k) \Delta t}{\omega(t_k)} I & \frac{1 - \cos \omega(t_k) \Delta t}{\omega(t_k)} I \\ 0 & \cos \omega(t_k) \Delta t I & \frac{\sin \omega(t_k) \Delta t}{\omega(t_k)} I \\ 0 & -\omega(t_k) \sin \omega(t_k) \Delta t I & \cos \omega(t_k) \Delta t I \end{bmatrix}_{9 \times 9} \quad (19)$$

It is possible that any of the three components of $\omega(t)$ would approach zero at any given instant in time. To computationally handle this it is necessary to take the limit of $\Phi(t_k, t_{k-1})$ as $\omega \rightarrow 0$; therefore,

$$\lim_{\omega \rightarrow 0} \Phi(t_k, t_{k-1}) = \begin{bmatrix} I & \Delta t I & \frac{\Delta t^2 I}{2} \\ 0 & I & \Delta t I \\ 0 & 0 & I \end{bmatrix}_{9 \times 9} \quad (20)$$

Note that in this model, the state transition matrix is time varying as opposed to the sampling frequency-dependent state transition matrix of the first filter model. For the purposes of this study, $\omega_i(t) < 0.01$ is assumed to be zero, $i = x, y, z$.

V. System Model with Constant Target Acceleration

For this model the nine filter states are the three components of relative position, relative velocity, and target acceleration. The differential state equations now are

$$\Delta \dot{S}(t) = \Delta V(t) \quad (21a)$$

$$\Delta \dot{V}(t) = A_T(t) - A_M(t) + w_M(t) \quad (21b)$$

$$\dot{A}_T(t) = w_T(t) \quad (21c)$$

The system model for the EKF now becomes:

$$\begin{bmatrix} \Delta \dot{S}(t) \\ \Delta \dot{V}(t) \\ \dot{A}_T(t) \end{bmatrix}_{9 \times 1} = \begin{bmatrix} 0 & I & 0 \\ 0 & 0 & I \\ 0 & 0 & 0 \end{bmatrix}_{9 \times 9} \begin{bmatrix} \Delta S(t) \\ \Delta V(t) \\ A_T(t) \end{bmatrix}_{9 \times 1} + \begin{bmatrix} 0 & 0 & 0 \\ 0 & I & 0 \\ 0 & 0 & 0 \end{bmatrix}_{9 \times 9} \begin{bmatrix} 0 \\ -A_M(t) \\ 0 \end{bmatrix}_{9 \times 1} + \begin{bmatrix} 0 \\ w_M(t) \\ w_T(t) \end{bmatrix}_{9 \times 1} \quad (22)$$

For the system model in Eq. (22) the state transition matrix [derived from Eq. (3)] is:

$$\Phi(t_k, t_{k-1}) = \begin{bmatrix} I & \Delta t I & \frac{\Delta t^2 I}{2} \\ 0 & I & \Delta t I \\ 0 & 0 & I \end{bmatrix}_{9 \times 9} \quad (23)$$

VI. System Model with Zero Target Acceleration

For this model the EKF is reduced to six states; the three components of relative position and relative velocity. The differential state equations are:

$$\Delta \dot{S}(t) = \Delta V(t) \quad (24a)$$

$$\Delta \dot{V}(t) = -A_M(t) + w_M(t) \quad (24b)$$

The system model for the EKF becomes:

$$\begin{bmatrix} \Delta \dot{S}(t) \\ \Delta \dot{V}(t) \end{bmatrix}_{6 \times 1} = \begin{bmatrix} 0 & I \\ 0 & 0 \end{bmatrix}_{6 \times 6} \begin{bmatrix} \Delta S(t) \\ \Delta V(t) \end{bmatrix}_{6 \times 1} + \begin{bmatrix} 0 & 0 \\ 0 & I \end{bmatrix}_{6 \times 6} \begin{bmatrix} 0 \\ -A_M(t) \end{bmatrix}_{6 \times 1} + \begin{bmatrix} 0 \\ w_M(t) \end{bmatrix}_{6 \times 1} \quad (25)$$

For the system model in Eq. (25), the state transition matrix is:

$$\Phi(t_k, t_{k-1}) = \begin{bmatrix} I & \Delta t I \\ 0 & I \end{bmatrix}_{6 \times 6} \quad (26)$$

VII. Measurement Model

The same measurement model was used for all four filter system models. The filter has two measurements: azimuth

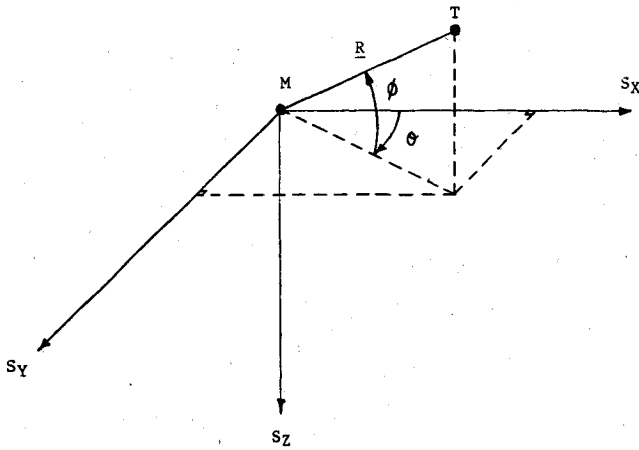


Fig. 1 Angular measurements related to filter states.

(ϕ) and elevation (σ) angle in inertial coordinates. The relationships between these angles and the filter's states is illustrated in Fig. 1.

The equations relating the angles to the filter states are

$$\phi = \tan^{-1}(-S_Z \sqrt{S_X^2 + S_Y^2}) \quad (27)$$

$$\sigma = \tan^{-1}(S_Y/S_X) \quad (28)$$

where S_X , S_Y , and S_Z are the three components of relative position in inertial coordinates. In state space format the measurement model is

$$\begin{bmatrix} \phi \\ \sigma \end{bmatrix}_{2 \times 1} = \begin{bmatrix} \tan^{-1}(-S_Z \sqrt{S_X^2 + S_Y^2}) \\ \tan^{-1}(S_Y/S_X) \end{bmatrix}_{2 \times 1} + \begin{bmatrix} v_{\phi_k} \\ v_{\sigma_k} \end{bmatrix}_{2 \times 1} \quad (29)$$

VIII. Noise Statistics and Filter Parameters

The same noise statistics and filter parameters were used for all four filter system models.

A. Noise Statistics

$$Q(t) = \begin{bmatrix} 0 & 0 & 0 \\ 0 & Q_M I & 0 \\ 0 & 0 & Q_T I \end{bmatrix}_{9 \times 9} \quad (30)$$

$$R_k = \begin{bmatrix} 0.25/R^2 + 5.625 \times 10^{-7} \\ 0.25/R^2 + 5.625 \times 10^{-7} \end{bmatrix} \quad (31)$$

B. Parameters

Q_M is the process noise covariance for missile acceleration. With an rms error of 0.4g for an accelerometer,

$$Q_M = [0.4(32.174 \text{ ft/s}^2)]^2 \quad (32)$$

Q_T is the process noise covariance for target acceleration. With an estimated variance on target acceleration of 20,000,

$$Q_T = 2P \quad (33)$$

Filter parameters are summarized in Table 1.

An additional input to the EKF is the initial conditions of the filter states and their variances. These values are listed in Table 2 (Ref. 3).

Table 1 Filter parameters

Parameters	Value
λ_T, s^{-1}	0.3
$Q_M, \text{ft}^2/\text{s}^4$	150
$Q_T, \text{ft}^2/\text{s}^4$	40,000
$\Delta t, \text{s}$	0.01

Table 2 Initial conditions

State	Mean	Variance
S_R	True value	10 ft ²
V_R	True value	10 ft ² /s ²
A_T	0 ft/s ²	20,000 ft ² /s ⁴

With a variance of 10 the filter is informed that the initial guess of relative position and velocity is within ± 3.16 ft (or ft/s) of its true value. With a variance of 20,000 the filter is informed that the initial guess of target acceleration is within ± 4.4 g of its true value.

IX. Guidance Law

The LQG guidance law used in the missile simulation is expressed in the following equations:

$$A_{M_X} = 3(S_{R_X}/t_{go}^2 + V_{R_X}/t_{go} + K_T A_{T_X}) \quad (34a)$$

$$A_{M_Y} = 3(S_{R_Y}/t_{go}^2 + V_{R_Y}/t_{go} + K_T A_{T_Y}) \quad (34b)$$

$$A_{M_Z} = 3(S_{R_Z}/t_{go}^2 + V_{R_Z}/t_{go} + K_T A_{T_Z}) \quad (34c)$$

The quantities appearing in the guidance law equations are described below.

$S_{R_X}, S_{R_Y}, S_{R_Z}$ = three components of relative position vector S_R referenced to the missile body, ft

$V_{R_X}, V_{R_Y}, V_{R_Z}$ = three components of relative velocity vector V_R referenced to the missile body, ft/s

$A_{T_X}, A_{T_Y}, A_{T_Z}$ = three components of target acceleration vector A_T referenced to the missile body, ft/s²

$A_{M_X}, A_{M_Y}, A_{M_Z}$ = three components of missile acceleration command vector A_M referenced to the missile body, ft/s²

K_T is the target acceleration gain, where

$$K_T = (e^{-\lambda_T t_{go}} - \lambda_T t_{go} + 1) / \lambda_T^2 t_{go}^2 \quad (35)$$

where T is the target acceleration response time coefficient, and t_{go} is the time to go, s (Ref. 2).

$$t_{go} = 2S_{R_X} / -V_{R_X} + \sqrt{V_{R_X}^2 + 4S_{R_X} A_{XX} / 3} \quad (36)$$

where A_{XX} is the difference between missile acceleration command and K_T times target acceleration in the axial direction, ft/s²

$$A_{XX} = A_{M_X} - K'_T A_{T_X} \quad (37)$$

and K'_T is K_T evaluated at the previous time interval.

$$K'_T = K_T |_{(t-\Delta t)} \quad (38)$$

The time-to-go algorithm has the advantage of explicitly accounting for the missile's axial acceleration, which has been ignored in the past; thus resulting in more optimal lateral and normal acceleration commands.

X. Performance Evaluation

An evaluation of the EKF with the four system models was conducted in two steps first, for a given missile/target engagement, graph of the percent errors in the filters estimates of the magnitude of relative position, relative velocity, and target acceleration vs time were generated for the four system models. For the model with the second-order Markov process, a graph of the percent errors in the estimates of target velocity replaced relative velocity. Graphs of the errors in the filters estimate of azimuth and elevation angles vs time were also generated for the four system models. This evaluation provides a measure of how well the filters estimate the states; however, a more effective evaluation is to determine how well the missile performs the EKF coupled with the LQG guidance law.

The second step of the performance evaluation involves the determination of miss distance (point of closest contact between the missile and target) for a specified number of initial launch conditions. For both evaluation steps a detailed six-degree-of-freedom (6-DOF) simulation of a generic bank-to-turn short-range air-to-air missile was used. The target used in the simulation incorporated a "smart" target algorithm incorporating a 9g out-of-plane evasive maneuver. The simulation contains detailed nonlinear math models of the major missile subsystems including the seeker, autopilot, and propulsion systems; realistic noise models of the onboard sensors and seeker models; detailed aerodynamic models of missile airframe characteristics; and the models that describe the missile's equations of motion. This missile/target combination was selected because it represents desired performance capabilities for the future guided weapons.

A. Estimation Error Graphs

For each of the EKF system models, the percent errors in the filter's estimates of the position, velocity, and acceleration magnitudes vs time were generated for the case of 0 deg off boresight (the off boresight angle defines the angle between the initial line-of-sight vector and the initial missile velocity vector, therefore, 0 deg off boresight means that the missile was launched pointing directly at the target) and 90 deg aspect angle (the angle between the initial line-of-sight vector and the target's velocity vector at launch). The initial launch range was 13,000 ft. The missile and target were coaltitude at launch (10,000 ft) and were cospeed at launch (0.9 Mach). The target performs its evasive out-of-plane maneuver when the range becomes less than 6000 ft. With 1 s left in the engagement, the target performs a dive, straight down. This launch condition was selected because it represents a challenging shot for the inertially referenced guidance and estimation algorithms.

Plots of the filters' estimation errors vs time provide graphic evidence of the ability or inability of the filter to estimate position, velocity, and acceleration during a single flyout in the presence of process and measurement noise. Figures 2-4 are a representative set of such plots for filter employing a first-order Markov process.

It should be noted that only the errors in magnitude coupled with errors in angle provide an effective evaluation of the filters' estimation capabilities. Large magnitude errors coupled with small angle errors indicate the filter maintains the proper ratios of the three components of position, velocity, and target acceleration, but does a poor job of estimating the overall magnitudes. On the other hand, small magnitude errors occurring simultaneously with large angle errors indicate the filter does not maintain the proper ratios of

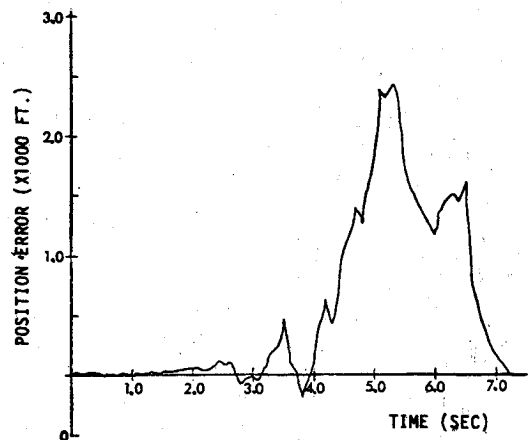


Fig. 2 Relative position error for first-order Markov filter.

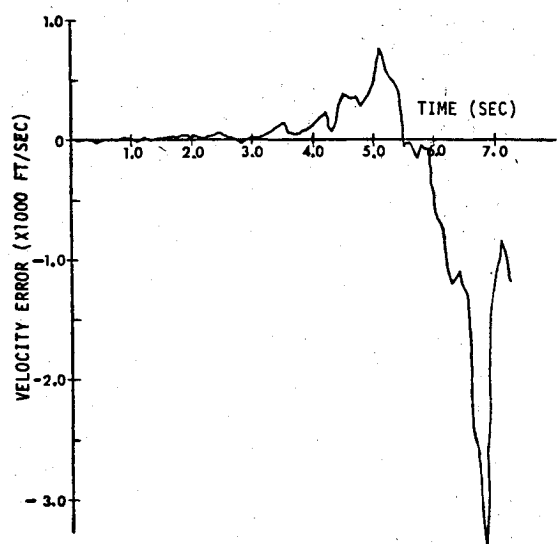


Fig. 3 Relative velocity error for first-order Markov filter.

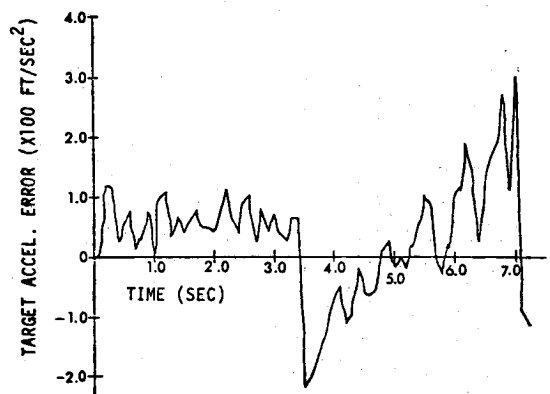


Fig. 4 Target acceleration error for first-order Markov filter.

the components of position, velocity, and acceleration but is successful at estimating the overall magnitudes. Sample plots of azimuth and elevation errors again for the first-order Markov filter are presented in Figs. 5 and 6.

B. Missile Performance

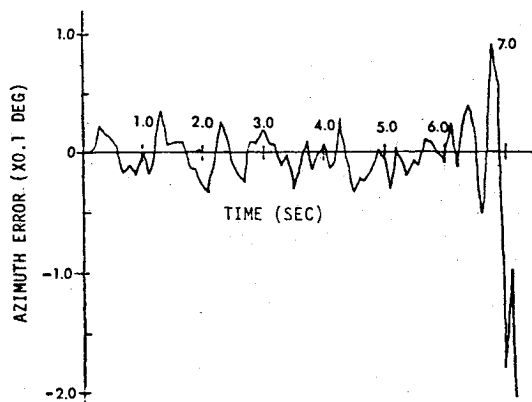
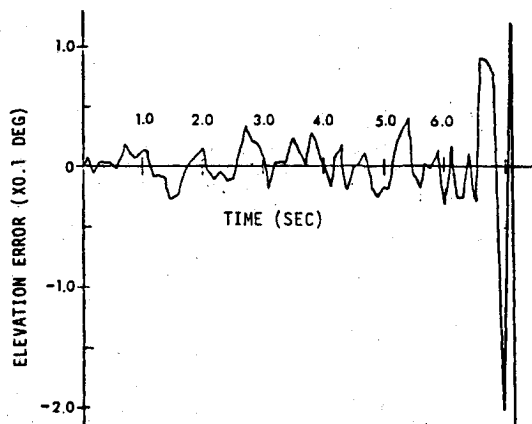
To evaluate the missile's performance with the EKF incorporating each of the four system models and the LQG guidance law defined in Sec. IV, numerous missile vs target flyouts were generated for a set of initial launch conditions listed in Table 3.

Table 3 Initial launch conditions

Launch condition	Launch range, ft	Launch aspect angle, deg	Launch off-boresight angle deg
1	8,000	0	0
2	13,000	90	0
3	26,000	180	0
4	7,500	0	40
5	11,000	90	40
6	24,000	180	40
7	1,000	45	0
8	3,000	135	0
9	1,000	45	40
10	2,500	135	40

Table 4 Average miss distance for each engagement

Launch condition	Miss distance, ft			
	Filter 1	Filter 2	Filter 3	Filter 4
1	5.73	4.74	4.63	418
2	7.00	5.83	6.03	192.4
3	4.81	7.46	6.10	256.8
4	13.09	9.73	9.90	742.8
5	7.85	6.88	11.46	270.1
6	3.00	10.50	11.45	296.0
7	3.55	17.40	3.61	16.3
8	11.60	10.25	10.10	8.4
9	2.01	13.54	2.10	59.3
0	4.61	14.49	5.21	7.5
Average miss distance	6.33	10.08	7.06	226.8

**Fig. 5 Azimuth angle error for first-order Markov filter.****Fig. 6 Elevation angle error for first-order Markov filter.**

The selection of these initial launch conditions was done such that the evaluation would provide a good sampling of the weapon's performance. The measurements were corrupted with the noise models defined in Sec. VIII. Since the noise models are random processes, it becomes necessary to fly repeated runs with different noise sequences for the same launch conditions (Monte Carlo analysis). Through some preliminary simulation analysis it was determined that 10 runs provide an accuracy in miss distance within 0.1 ft, which is adequate for the purposes of this study. The results presented in this section are based on the use of 10 Monte Carlo runs and are illustrated in Table 4. The miss distance is calculated as the mean miss distance over the 10 Monte Carlo runs. Filter 1 incorporates the first-order Markov process, filter 2 incorporates the second-order Markov process, filter 3 incorporates the constant target acceleration model, and filter 4 incorporates the zero target acceleration model.

XI. Results

The results of the estimation error vs time plots for each of the candidate filters indicate that they all do a poor job of estimating the states with only passive seeker information in highly dynamic environment. The errors resulting from the first-order Markov filter are very similar to those from the constant acceleration filter. Both produce small relative position and velocity errors until the target begins maneuvering. Velocity errors begin to grow following the first 9g target maneuver, are corrected in approximately 2 s then grow again, in the opposite direction when the target performs its final 9g dive. The velocity error is again largely corrected before the end of the engagement. Position errors for both filters grow as the target begins to maneuver but are corrected before the engagement ends. With both the first-order Markov and constant acceleration filters, the target acceleration estimates are oscillatory and overestimated when the target is not maneuvering. When the target begins its maneuver, target acceleration is initially underestimated. The filters recover and soon overestimate target acceleration again. The oscillations continue to grow and are quite large near the end of the engagement.

The state estimation errors produced by the second-order Markov filter are quite different from either of two filters discussed above. Estimates of relative position and velocity begin diverging immediately.

The position error peaks at nearly 4000 ft and is entirely corrected during the last 2 s of the engagement. Velocity estimate error continues to diverge, however, throughout the flight. Target acceleration errors are more oscillatory than those from the Markov filters. It is important to note that for both the two Markov filters and the constant acceleration filters, the errors in azimuth and elevation angles are relatively small until the last 0.5 s of the engagement at which point they diverge rapidly.

The velocity and position estimation errors from the zero acceleration filter are small until the target begins to maneuver. Even then, these errors never grow as large as for the other filters and they are corrected by the filter before the engagement ends. However, the errors in azimuth and elevation angles resulting from this filter become large as the target begins to maneuver and, as the final target dive is executed, the angle errors diverge rapidly. This results in the large misses listed in Table 4.

These results clearly indicate a deficiency in the EKF's ability to estimate relative position, velocity, and target acceleration with passive seeker information. However, the filter's true effectiveness is measured in terms of missile performance using the LQG guidance law coupled with the EKF. The results in Table 4 indicate that the missile performs well with all the filters except the one using the zero acceleration model. The differences in missile performance with the first-order Markov, second-order Markov, and constant acceleration filters are not substantial, except that missile with

the second-order Markov filter does not perform as well as the other two for close-in shots. The zero acceleration filter results in very poor performance except under near head-on, short launch range conditions.

XII. Conclusions

The relative merits of the acceleration models are based not only on the performance of the resulting filter but also upon their complexity and resulting computational burden. While the performance of the first-order Markov and constant acceleration filters are similar, the first-order Markov model results in more complex state transition matrix. This becomes a factor for weapon systems require variable sampling rates because the state transition matrix must then be calculated online. The second-order Markov filter performs slightly worse than either of the above two and imposes a much more severe computational burden for two reasons. First, a time varying state transition matrix results which must be computed at each sample period. Second, additional complexity is required to prevent singularity when target turning rate approaches zero. The inability of the zero acceleration model to maintain proper position and velocity angles and the resulting poor missile performance make it unacceptable for use against a highly maneuverable target.

This study was conducted to evaluate several methods for modeling target acceleration in an extended Kalman filter, and, by no means, are any of the four filters considered to be

"the" answer to the tactical missile guidance problem. Estimating position, velocity and acceleration from angle-only information is a very difficult problem. While Kalman filtering offers the most effective near term solution, the accuracy of the state estimates obtained to date leave much room for improvement. Even so, previous studies have shown that a linear quadratic guidance law coupled with an extended Kalman filter working on angle only information provides a significant missile performance improvements over conventional proportional navigation in highly dynamic engagements.

References

- ¹ Pastrick, N.L., Seltzer, S.M., and Warren, M.E., "Guidance Laws for Short-Range Tactical Missiles," *Journal of Guidance and Control*, Vol. 20, March-April 1981, pp. 98-108.
- ² McClendon, J.R., and Vergez, P.L., "Applications of Modern Control and Estimation Theory to the Guidance of Tactical Air-to-Air Missiles," *Proceedings of the Second Meeting of the Coordinating Group on Modern Control Theory*, Aberdeen Proving Grounds, Md., Dec. 1980.
- ³ Sammons, J.M., Balakrishnan, S., Speyer, J.L., and Hull, D.G., "Development and Comparison of Optimal Filters," AFATL-TR-79-87, Oct. 1979.
- ⁴ Anderson, G.M., "Guidance and Control Law Methodology," AFATL-TR-79-86, Oct. 1979.
- ⁵ Fuller, J.W. et al., "Tactical Missile Guidance and Control Law Methodology," AFATL-TR-80-144, Oct. 1980.

From the AIAA Progress in Astronautics and Aeronautics Series...

EXPLORATION OF THE OUTER SOLAR SYSTEM—v. 50

Edited by Eugene W. Greenstadt, Murray Dryer, and Devrie S. Intriligator

During the past decade, propelled by the growing capability of the advanced nations of the world to rocket-launch space vehicles on precise interplanetary paths beyond Earth, strong scientific interest has developed in reaching the outer solar system in order to explore in detail many important physical features that simply cannot be determined by conventional astrophysical observation from Earth. The scientifically exciting exploration strategy for the outer solar system—planets beyond Mars, comets, and the interplanetary medium—has been outlined by NASA for the next decade that includes ten or more planet fly-bys, orbiters, and entry vehicles launched to reach Jupiter, Saturn, and Uranus; and still more launchings are in the initial planning stages.

This volume of the AIAA Progress in Astronautics and Aeronautics series offers a collection of original articles on the first results of such outer solar system exploration. It encompasses three distinct fields of inquiry: the major planets and satellites beyond Mars, comets entering the solar system, and the interplanetary medium containing mainly the particle emanations from the Sun.

Astrophysicists interested in outer solar system phenomena and astronautical engineers concerned with advanced scientific spacecraft will find the book worthy of study. It is recommended also as background to those who will participate in the planning of future solar system missions, particularly as the advent of the forthcoming Space Shuttle opens up new capabilities for such space explorations.

251 pp., 6x9, illus., \$15.00 Member \$24.00 List

TO ORDER WRITE: Publications Order Dept., AIAA, 1633 Broadway, New York, N.Y. 10019